

An absolutely stable open time crystal

Quntao Zhuang^{1,2,*}, Francisco Machado^{1,3,*}, Norman Y. Yao^{1,3}, and Michael P. Zaletel^{1,3}

¹*Department of Physics, University of California, Berkeley, California 94720, USA*

²*Department of Electrical and Computer Engineering & James C. Wyant College of Optical Sciences, University of Arizona, Tucson, Arizona 85721, USA*

³*Materials Science Division, Lawrence Berkeley National Laboratory, Berkeley, California 94720, USA*

(Dated: October 5, 2021)

We show that locally-interacting, periodically-driven (Floquet) Hamiltonian dynamics coupled to a Langevin bath support finite-temperature discrete time crystals with an infinite auto-correlation time. The time crystalline order is stable to arbitrary perturbations, including those that break the time translation symmetry of the underlying drive. Our approach utilizes a general mapping from probabilistic cellular automata (PCA) to open classical Floquet systems. Applying this mapping to a variant of the Toom cellular automata, which we dub the “ π -Toom PCA”, leads to a 2D Floquet Hamiltonian with a finite-temperature period-doubling phase transition. We provide numerical evidence for the existence of this transition, and analyze the statistics of the finite temperature fluctuations. Finally, we discuss how general results from the field of probabilistic cellular automata imply the existence of discrete time crystals in all dimensions, $D \geq 1$.

I. INTRODUCTION

A tremendous amount of recent excitement has centered upon interacting periodically-driven (Floquet) “phases of matter” [1–7]. While discussed as non-equilibrium phases, thus far attention has largely focused on two scenarios which are non-equilibrium only in a rather restricted sense. First, there are quantum “many-body-localized” (MBL) Floquet phases [2–4, 8–11]. Because the ergodicity breaking of MBL is sufficient to prevent the periodic drive from heating the system to infinite temperature, the system does not need to be coupled to a dissipative bath (e.g., the dynamics are driven, but purely unitary) [12–14]. In this case, the eigenstates of the Floquet evolution have area-law entanglement, which allows much of the physics to be mapped to more familiar questions of order in quantum ground states [15–18]. Second, there are “prethermal” Floquet phases which heat only exponentially slowly due to (for example) a mismatch between the driving frequency and the natural frequencies of the undriven system [19–28]. During the exponentially long time-scale before heating, these systems can exhibit behavior which is analogous to order in finite temperature equilibrium phases [20, 24, 26, 27]. However, prethermal Floquet phases are not “true” phases in the strict sense because they are distinguished from disordered behavior via crossovers, rather than sharp transitions [7].

Perhaps the most paradigmatic example of a Floquet phase of matter is the so-called discrete time-crystal (DTC)—starting from a generic initial state, at long times the DTC relaxes into a steady state with a temporal periodicity which is a multiple of the drive’s [2–4]. This behavior is stable to small perturbations of the dynamics that respect the underlying time-translation symmetry of the drive, and thus, is “rigid” in the usual sense

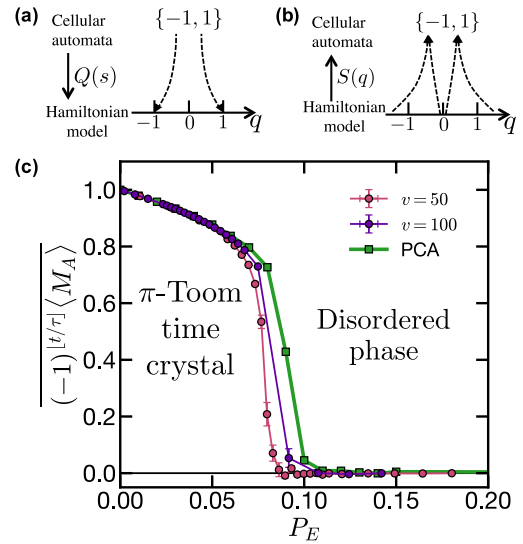


Figure 1. (a,b) Schematic of the translation between the discrete state space of a cellular automata and the continuous state space of a Hamiltonian model. (c) Time crystalline order parameter (e.g. stroboscopic magnetization) as a function of the error probability. The phase transition from a discrete time crystal to the disordered phase is shown for both a Floquet Langevin simulation of the π -Toom model with pinning potential $v = 50, 100$, as well as for a direct implementation of the probabilistic cellular automata.

that a phase of matter is. Similar behavior has been studied in the non-linear dynamics community as either “subharmonic entrainment” or “asymptotic periodicity” [29–33]; for a discussion of how this earlier work differs from results in the quantum many-body context, we refer the reader to [7, 34, 35].

It is natural to ask if “true” time-crystals exist beyond MBL. Without MBL to prevent heating, stabilizing time crystalline order presumably require coupling to a dissipative bath. Combining periodic driving and

* These two authors contributed equally

a dissipative bath introduces the full complexity of non-equilibrium dynamics.

Thinking microscopically, classical driven dissipative systems are described by Hamiltonian dynamics coupled to a finite-temperature Langevin bath, or in the quantum case, periodically driven Lindbladian evolution. A key feature of both these contexts is that if the bath is dissipative, at finite temperature it should also come with noise due to the fluctuation-dissipation theorem; at zero temperature, where there is damping but no noise, many-body time-crystals can occur rather trivially by analogy to the “period doubling” of coupled iterated logistic maps [36–40]. The key question we will focus on is the following: Can true time-crystals exist in a periodically driven system of locally interacting particles coupled to an equilibrium bath at finite temperature?

In this work, we argue in the affirmative: finite-temperature time-crystals, with an *infinite* auto-correlation time, can exist even in translation-invariant arrays of classical non-linear oscillators interacting only with their nearest-neighbors. To do so, we leverage non-trivial results in the field of probabilistic cellular automata (PCA) [41, 42]. A PCA is a deterministic cellular automata (CA) perturbed by stochastic errors, mimicking the effect of finite temperature, making it a “stripped-down” model of finite-temperature non-equilibrium dynamics. We first use the results of Gács (1D) [43, 44] and Toom (2D) [45–47] to show that local PCAs can exhibit time-crystalline behavior stable to arbitrary small perturbations. Unlike MBL or prethermal time crystals, such time-crystalline order is “absolutely stable”, in the sense that it remains robust *even* in the presence of perturbations that break the discrete time-translation symmetry of the periodic drive.

However, one may wonder whether this result extends to the physical setting of interest — classical Langevin dynamics — which is constrained, for example, by symplectic structure and the fluctuation-dissipation theorem. To this end, we show how classical Langevin dynamics can be used to “simulate” any PCA, and further provide numerical evidence that the errors due to Langevin noise are of a type covered by Gács’ and Toom’s mathematical results. Applying this to a 2D array of locally interacting mechanical oscillators, Langevin simulations reveal a finite-temperature phase transition between a discrete time-crystal and a disordered phase.

II. TIME-CRYSTALS IN A PCA: THE π -TOOM AND π -GÁCS MODELS

We begin by reviewing the definition of a PCA, and explain how the results of Gács and Toom imply the existence of time-crystals in this setting [43–45, 48]. As in a CA, the state of a PCA is given by a spin configuration $\{\eta(x)\}$, where $x \in \Lambda$ labels sites in a regular lattice Λ and each $\eta(x)$ takes values in a set $\mathcal{S} = \{1, 2, \dots, d\}$. In a CA, the dynamics are governed by a deterministic

transition rule [49, 50],

$$\{\eta(\mathbf{x}, t + 1)\} = \mathcal{T}\{\{\eta(\mathbf{x}, t)\}\} \quad (1)$$

[Fig. 2(a)]. In a PCA, the spins instead evolve under a Markov process described by the transition matrix $M_{\eta \rightarrow \eta'}$, which characterizes the *probability* to evolve from configuration η to η' [51–53]. M should be local in the sense that the update distribution of a spin depends only on the state of its nearest neighbors, or more generally, on some finite range “neighborhood” \mathcal{N} .

A particularly natural class of PCAs arise by starting with a deterministic CA and perturbing it with an “error rate” ϵ . More concretely, at each step, the spins first follow the rule \mathcal{T} , and then with a probability bounded by ϵ they randomly flip to a different state. One can think of the resulting Markov process as a perturbation to the deterministic one, $M = \mathcal{T} + \epsilon \Delta M$, where ΔM determines the precise error distribution. The mathematical results we will describe can in fact account for even more general (non-Markovian) error models, as we will describe shortly [43, 54].

A deterministic CA (with $\mathcal{S} = \{-1, 1\}$) can trivially realize a time-crystal: for example, the rule $1 \leftrightarrow -1$. In fact, since CA are capable of universal classical computation, they can realize any dynamical phenomena which can be programmed on a computer [55]. Whether a PCA can realize a stable time-crystal is significantly more subtle. The long-time dynamics of a PCA are described by the stationary probability distributions $\mathcal{P}[\eta]$ of M , e.g., $M\mathcal{P}[\eta] = \mathcal{P}[\eta]$. We say M exhibits an n -fold subharmonic response if there are $n > 1$ distinct distributions, $\mathcal{P}_i[\eta]$, such that $M\mathcal{P}_i[\eta] = \mathcal{P}_{i+1}[\eta]$, with $\mathcal{P}_n = \mathcal{P}_0$. This simply formalizes the notion of long-time oscillations: at long times a generic initial state will relax into to a non-uniform convex combination $\sum_i p_i \mathcal{P}_i$ which is stationary under M^n , but not M . Such behavior has also been referred to as asymptotic periodicity [29]. A time crystal is then defined to be a local PCA with a *stable* n -fold subharmonic response: for sufficiently small but arbitrary local perturbations ΔM , $M + \Delta M$ should retain its n -fold subharmonic response. This motivates the following sharp question: Do PCA time crystals exist [56]?

If we perturb the CA rule, $1 \leftrightarrow -1$, with random errors at rate ϵ , it is not a time-crystal: over a time-scale $\sim 1/\epsilon$, each spin will forget its initial state and relax to the maximally mixed distribution. One could try and fix this by adding some local interactions: for example, each site transitions to state η if a majority of its neighbors are in the state $-\eta$. While this simple “error-correction” procedure can increase the relaxation time relative to $\sim 1/\epsilon$, it is known that the relaxation time remains finite [44]. A more sophisticated approach is required.

Ergodicity breaking in a PCA—One prerequisite for a time-crystal is ergodicity breaking. A PCA is “ergodic” if it has a unique stationary distribution, so that at long times the state is independent of the initial spin configuration. A time-crystal necessarily breaks ergodicity because M^n has n stationary distributions, so the sys-

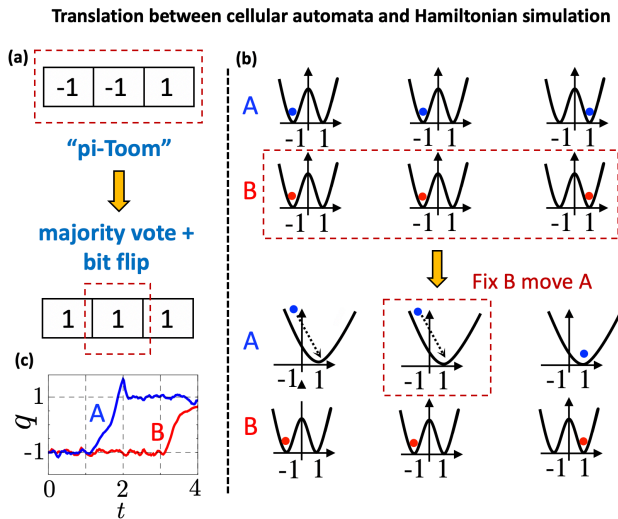


Figure 2. Schematic depicting the translation between a cellular automata step and the corresponding Hamiltonian simulation step. (a) Shows a single step of a one dimensional version of the “ π -Toom” rule, which consists of a majority vote and a bit flip. (b) In the Hamiltonian setting, we consider two sets of oscillators, A (blue) and B (red). The corresponding Hamiltonian simulation proceeds in two steps. First, there is a “relaxation” step followed by local interactions which implement the “majority vote”. In this second step, the B oscillators are fixed, while the state of the A oscillators is updated. (c) Trajectory $q_{A/B}(t)$ during an error correction step of the Toom model for a 32×32 lattice with $v = 50$ and $T = 2$. The vertical dashed lines divide time into four steps as described in the text; an error of the form $q \sim -1$ gets corrected to be $q \sim 1$.

tem remembers which of the n states in the orbit it is in.

Ergodicity-breaking PCAs were first proved to exist in 2D by Toom [45, 51], and much later in 1D by Gács [43]. Since stable ergodicity breaking is impossible in a zero dimensional model with a finite state space [57, 58], the results of Toom and Gács necessarily require interactions and dimension $D \geq 1$ (to take the thermodynamic limit). We discuss Toom’s model first because of its simplicity. The Toom model is a 2D CA with a binary state space, $\mathcal{S} = \{-1, 1\}$, and a “majority vote” transition rule in the Northern-Eastern-Center (NEC) neighborhood $\mathcal{N} = \{(1, 0), (0, 1), (0, 0)\}$ (the $(\Delta x_i, \Delta y_i) \in \mathcal{N}$ denote the relative locations of the cells in the neighborhood). Namely, the new state of cell \mathbf{x} is determined by the majority value of the three NEC neighbors, $\mathbf{x} + \mathcal{N}$. Crucially, in this model, it was proven that there are two “phases” (i.e. stationary distributions), corresponding to states “all +1” and “all -1”, which are stable against arbitrary stochastic perturbations below a critical error rate ϵ . The origin of this stability can be intuitively understood: without any errors, the NEC majority vote eliminates any finite island of errors in a short time; as long as the error rate ϵ is small enough, the system can elim-

inate an island before another equally large island appears [46, 47, 54].

We emphasize that the coexistence of two stable phases in the Toom model is of a much *stronger* nature than the coexistence of equilibrium phases (i.e. all up and all down) in, for example, the 2D Ising model; this is because the coexistence in the Toom model is stable even if the errors are *biased*. For example, while the deterministic Toom CA happens to have a transition rule with an Ising symmetry, one can perturb using two different error rates, $\epsilon_1 < \epsilon_{-1}$, for states to flip to ± 1 , respectively. Despite this bias, at long times, two separate stationary distributions $\mathcal{P}_+, \mathcal{P}_-$ persist. This is in contrast to equilibrium systems (i.e. the 2D Ising model), where coexistence is always fine-tuned, either via a symmetry, or by tuning to the boundary of a first order phase transition.

With Toom having done the hard part, a simple modification we call the “ π -Toom” model turns his construction into a time-crystal: instead of an NEC majority vote, we take as our rule the NEC anti-majority vote. Or equivalently, we consider the model in which we interleave a spin flip, $1 \leftrightarrow -1$, between each Toom step. Because Toom has proved that his construction can successfully “error-correct” against minority islands, one can immediately conclude the π -Toom model is a period-doubled time-crystal below a critical error rate ϵ , even if the noise breaks the Ising symmetry. Above this error rate, there is a transition into a disordered phase, analogous to the ergodicity-breaking phase transition of the Toom model. We will numerically confirm this transition exists in the π -Toom model in Section IV. We note that the potential for the Toom rule to stabilize periodic behavior in PCAs was pointed out well before the recent interest in time-crystals [32, 56].

Time crystalline order in a 1D PCA—As with conventional phases of matter, the possibility of a stable, discrete time crystal depends on spatial dimension. Thus, it is natural and interesting to ask if a PCA time-crystal can also exist in 1D. Note that in the quantum case, while the 1D MBL discrete time crystal is fairly well established [2–4, 59, 60], the stability of MBL in 2D, and hence the existence of a 2D MBL DTC phase, remains controversial [61, 62].

Unfortunately, Toom’s route to stability cannot be generalized to 1D. Since each island of errors is only separated by two domain walls in one dimension, locally one cannot efficiently tell which side corresponds to the error and which side to the correct region. This intuition is not specific to the Toom model, and in fact for many decades it was conjectured that all 1D, finite-range and finite-state PCAs were generically ergodic, i.e. the so-called “positive-rates conjecture” [44].

Surprisingly, in 1998, this longstanding conjecture was proven incorrect by Gács [43]. Gács constructed a 1D translation invariant PCA, with nearest neighbor interactions, with the following remarkable property: on a chain of length L , the dynamics exhibit 2^L stable stationary measures (intuitively, one can think of these as fixed

points) in the limit $L \rightarrow \infty$; said another way, Gács' PCA can "remember" one bit per unit length! Each cell/site of the PCA has a large state space, likely somewhere between 2^{24} and 2^{400} [43, 44]. Roughly speaking, each cell contains one bit that it is trying to remember, and the remaining 399 bits (taking e.g. the 2^{400} state space) are involved in a highly collective error correction protocol. As in the Toom model, the stochastic errors can be biased so long as they remain below some finite threshold, above which a dynamical phase transition will restore ergodicity.

Even more remarkably, not only is the Gács model an error-corrected memory, it can execute Turing-complete operations on the protected state space. In other words, his construction demonstrates that a *stochastic* 1D PCA can be used to simulate a deterministic CA, and hence error-corrected classical computing is possible in 1D. This immediately implies the existence of the " π -Gács time crystal." In particular, one can simply use the Gács construction to emulate a CA with the rule: $1 \leftrightarrow -1$. His mathematical results then imply that this is an absolutely stable discrete time crystal, with infinitely long-lived temporal order as $L \rightarrow \infty$.

Gács' result (and Toom's) is mathematically rigorous, and as such, there are assumptions about the error model, which we outline here [43, 45, 54]. Since the PCA is viewed as a perturbation to a CA rule \mathcal{T} , given a particular spatio-temporal history $\eta(\mathbf{x}, t)$, we say an "error" E_u occurred at space-time point u if it didn't follow the update rule \mathcal{T} ; instead, the state of u is chosen according to some noise distribution. $E_{u_1} \wedge E_{u_2}$ then denotes the situation where errors have occurred at both u_1 and u_2 . Gács only requires that the probability that errors (of any type) occurring at k space-time points $\{u_\ell\}$ satisfy the bound $P_{\bigwedge_{\ell=1}^k E_{u_\ell}} \leq \epsilon^k$ for some constant ϵ [43]. The Gács model is non-ergodic below a finite critical ϵ , *irrespective* of the further details of $P_{\bigwedge_{\ell} E_{u_\ell}}$. Thus, Gács' error model is extremely general — it does not even require that the errors come from a Markov process.

To understand why most physical systems would naturally satisfy this bound, one can expand Gács' error condition using the chain rule for conditional probabilities, $P_{X \wedge Y} = P_{X|Y}P_Y$, which yields

$$P_{\bigwedge_{\ell=1}^k E_{u_\ell}} = \prod_{\ell=1}^k P_{E_\ell | E_{\ell-1} \dots E_1} \leq \epsilon^k. \quad (2)$$

Thus, a sufficient condition is simply to require that each $P_{E_\ell | E_{\ell-1} \dots E_1} \leq \epsilon$; if we choose ℓ to be ordered in time, this will be satisfied if the probability for an error to occur at ℓ , conditioned on all of the past errors, is below some constant ϵ . This will *always* be the case for a Markov model of the form, $M = \mathcal{T} + \epsilon \Delta M$, for arbitrary (local) entries $|\Delta M_{\eta \rightarrow \eta'}| < 1$. Thus, the "stability to errors" of the Gács model can be understood, more generally, as the stability to local perturbations.

III. TRANSLATING A PCA INTO FLOQUET-LANGEVIN DYNAMICS

Our goal in this section is to bridge the gap between the preceding results from theoretical computer science and systems more familiar to many-body physics. Specifically, we aim to map the π -Toom and π -Gács models to a classical Floquet Hamiltonian coupled to a Langevin bath which instantaneously satisfies detailed balance. A well-known mapping from D -dimensional CA to $D + 1$ -dimensional *equilibrium* models was studied in the 1980s [46, 63, 64]; however, these mappings introduce an extra spatial dimension corresponding to the history of the CA. Thus, time-translation breaking in the original CA does not actually give rise to time-crystalline order in the resulting Hamiltonian.

So here we take a different approach. We should say at the outset that there is nothing particularly special about our strategy, and other proposals may work equally well. In fact the problem can be understood as a constrained instance of the well-studied "embedding problem:" we aim to realize a discrete-time Markov process (the PCA) via the stroboscopic dynamics of a continuous time Monte Carlo chain (CTMC) satisfying local detailed balance (LDB) [65–67].

The dynamics we consider take the general Langevin form,

$$\begin{aligned} \dot{q}_i &= \partial_{p_i} H(\{p, q\}; t) \\ \dot{p}_i &= -\partial_{q_i} H(\{p, q\}; t) + R_i(t) - \gamma p_i \\ \langle R_i(t) R_j(t') \rangle_{\text{noise}} &= 2\gamma T \delta_{ij} \delta(t - t'), \end{aligned} \quad (3)$$

where (q_i, p_i) are the conjugate variables of a mechanical oscillator at site i . As depicted in Fig. 1(a,b), roughly speaking we will encode the discrete state of the CA spin, η_i , as the integer part of the position, $\eta_i = \lfloor q_i \rfloor$. The Hamiltonian will take the familiar form $H(t) = \sum_i \frac{p_i^2}{2m} + U(\{q\}, t)$, with $U(t)$ engineered so that one Floquet cycle, $H(t + \tau) = H(t)$, will enact one cycle of the CA update \mathcal{T} . In order to satisfy the fluctuation-dissipation theorem at each instant in time, $R_i(t)$ is a stochastic force whose variance is proportional to the friction coefficient γ and the temperature T . This stochastic force will sometimes lead to "errors" in the Hamiltonian simulation of the CA, making it effectively a PCA.

Let us begin by defining the precise mapping between the state s of a single spin in the CA and the phase space (q, p) of a single oscillator. Each spin takes on values within the discrete state space \mathcal{S} , while the oscillators take on continuous values, $q \in \mathbb{R}$. To map from the CA to the oscillator ($Q : \mathcal{S} \rightarrow \mathbb{R}$), we use $Q(s) = s$ [Fig. 1(a)]. To map from the oscillator to the CA ($S : \mathbb{R} \rightarrow \mathcal{S}$), we use the following prescription: given a position q , the corresponding state $S(q) = s$ is given by the closest $Q(s)$ such that $S(q) = \arg \min_s |Q(s) - q|$ [Fig. 1(b)]. We note that the oscillator-to-CA mapping is many-to-one; indeed, it is completely independent of the momentum p .

When building Hamiltonian dynamics that simulate

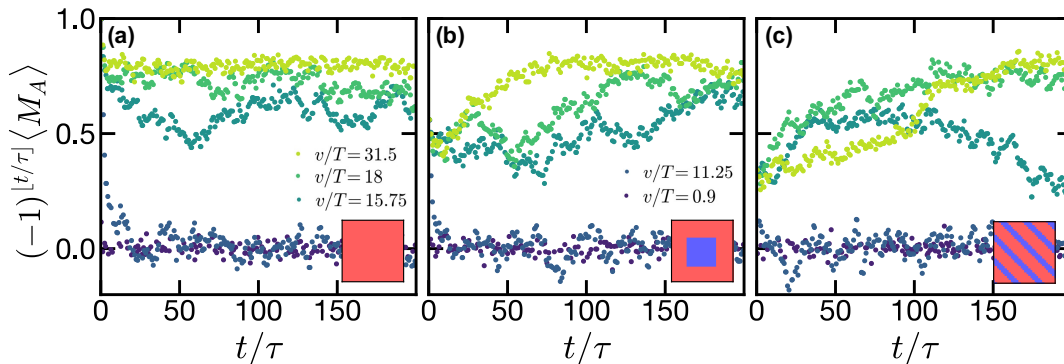


Figure 3. Floquet Langevin simulation of the π -Toom model for a two dimensional lattice of size 32×32 , with $v = 50$. For each panel, the inset depicts the initial configuration (for both A and B oscillators), where red indicates $q = +1$ and blue indicates $q = -1$. (a) For a uniform initial state, at low temperatures, the time crystalline order parameter remains finite at late times. At high temperatures, the time crystal quickly melts into a disordered phase. (b) For an initial state with a central island of errors (i.e. oscillators in $q = -1$), at low temperatures, the Floquet Langevin dynamics “error correct” and the time crystalline order grows toward a plateau at late times. At high temperatures, the time crystal again melts into a disordered phase. (c) For an initial state with stripes of errors, one sees the same qualitative behavior as in panel (b). As expected, near the transition (data set with $v/T = 15.75$), it becomes difficult to tell whether the time crystalline order will eventually decay or plateau to a finite value.

the CA, we encounter a challenge. Unlike the discrete time evolution of the CA, where the update of the global state is immediate, in a continuous-time Hamiltonian system, one needs a way to “store” the previous global state throughout the update cycle. This is essential in order to give the dynamics enough time to identify what the new state of the system should be. To solve this issue, we promote each CA cell at position \mathbf{x} to *two* oscillators (A and B) with coordinates $(q_{\mathbf{x}}^A, p_{\mathbf{x}}^A)$, and $(q_{\mathbf{x}}^B, p_{\mathbf{x}}^B)$. At each step, we will view one set of oscillators (say A) as the “memory”, while the other set (B) will undergo evolution to the new state $B = \mathcal{T}(A)$, driven by $U(t)$. We then exchange the role of A and B and repeat. In a sense, our protocol condenses the extra history dimension of the equilibrium construction [46, 63, 64] to a constant overhead in the state-space size. Interestingly, it was recently shown that such ancillary “hidden” degrees of freedom are necessary in any CTMC realization of a sufficiently non-trivial discrete-time Markov chain, including the “bit-flip” process (e.g. a time-crystal) [67].

Within this protocol, one Floquet cycle ($A \rightarrow B \rightarrow A$) can actually execute *two* CA steps. However, when considering discrete time-crystals, where we want the Floquet period to enact a single CA step, one can always make one of the steps equivalent to either the “do-nothing” (\mathcal{I}) or Toom CAs. This would result in an interleaving of the form: $(\mathcal{I}\mathcal{T})(\mathcal{I}\mathcal{T}) \dots$.

Building the Floquet dynamics—We now turn to building the Floquet dynamics, which simulate the transition rules of the cellular automata. We begin with the oscillators at site \mathbf{x} in the state $(q_{\mathbf{x}}^{A/B}, p_{\mathbf{x}}^{A/B}) = (Q(\eta(\mathbf{x}, t)), 0)$. From there, the dynamics evolve via a 4-step process.

Step 1: Relaxation. The goal of the first step is to leverage dissipation in order to reduce fluctuations in

the system. In particular, we envision turning on a one-body potential, $V_{\text{pin}}(q)$, which has a local minimum at $Q(s)$ for all $s \in \mathcal{S}$. At sufficiently low temperatures, the dissipative dynamics [Eqn. 3] will relax the oscillator’s positions, $q_{\mathbf{x}}$, toward valid values of $Q(s)$ with low momenta (with fluctuations of order the equipartition scale $\sim k_B T$). The precise form of V_{pin} is not important; however, for concreteness we will utilize

$$V_{\text{pin}}(q) = v_{\text{pin}} \prod_{s \in \mathcal{S}} (Q(s) - q)^2 \quad (4)$$

where the overall magnitude of the pinning potential is set by v_{pin} .

Step 2: Fix A move B. As illustrated in Fig. 2, the second step of the Floquet dynamics implements the cellular automata transition $B = \mathcal{T}(A)$. We will keep q^A fixed using the pinning potential, V_{pin} . For the B oscillators, however, we turn off V_{pin} , and turn on an interaction V_I between q^A and q^B . This interaction is engineered such that each $q_{\mathbf{x}}^B$ sees only a single potential minimum corresponding to the desired CA update rule; in general, this will depend on the state of the A oscillators in the associated neighborhood, $\{q_{\mathbf{x}+\mathcal{N}}^A\}$.

Defining the location of this minimum to be $\tilde{\mathcal{T}}(\{q_{\mathbf{x}+\mathcal{N}}^A\})$, we can then specify an interaction of the form:

$$V_I(\{q_{\mathbf{x}+\mathcal{N}}^A\}, q_{\mathbf{x}}^B) = \frac{v_I}{2} \left(\tilde{\mathcal{T}}(\{q_{\mathbf{x}+\mathcal{N}}^A\}) - q_{\mathbf{x}}^B \right)^2, \quad (5)$$

where the interaction strength is characterized by v_I . This is a highly non-linear but local interaction between each $q_{\mathbf{x}}^B$ and a finite set of A oscillators, $\{q_{\mathbf{x}+\mathcal{N}}^A\}$, within the neighborhood, \mathcal{N} . In particular, as shown in Fig. 2(b), for the example of $\tilde{\mathcal{T}}$ being an “anti-majority

vote”, the interaction would correspond to an $|\mathcal{N}| + 1$ body coupling [68].

Step 3: Relaxation. In the third step, we turn off the interaction, V_I , while ramping up the pinning potential, V_{pin} . As in the first step, dissipation relaxes and pins the positions of the oscillators.

Step 4: Fix B move A. In the final step, we implement “ $A = \mathcal{T}(B)$ ” by repeating step two with the role of A and B reversed.

After these four steps, our Floquet dynamics have implemented two steps of the cellular automata update rule, \mathcal{T} . This block naturally forms a single period of the Floquet drive, which can then be repeated. As aforementioned, one can also replace the transition \mathcal{T} in step two with the “do-nothing” CA rule if one wants to implement only a single CA update, \mathcal{T} , per Floquet cycle.

We now have all of the ingredients to explicitly define our Langevin dynamics, governed by:

$$H(t) = \sum_{\mathbf{x}} \frac{p_{\mathbf{x}}^{A^2}}{2m} + \frac{p_{\mathbf{x}}^{B^2}}{2m} + U(t, \{q_{\mathbf{x}}^A, q_{\mathbf{x}}^B\}), \quad (6)$$

where the potential $U(t, \{q_{\mathbf{x}}^A, q_{\mathbf{x}}^B\})$ has a Floquet period of $\tau = 4$:

$$U(t, \{q_k^A, q_k^B\}) = \begin{cases} \sum_{\mathbf{x}} V_{\text{pin}}(q_{\mathbf{x}}^A) + V_{\text{pin}}(q_{\mathbf{x}}^B) & \text{if } \text{mod}(\lfloor t \rfloor, 4) = 0, 2; \\ \sum_{\mathbf{x}} V_{\text{pin}}(q_{\mathbf{x}}^A) + V_I(q_{\mathbf{x}+\mathcal{N}}^A, q_{\mathbf{x}}^B) & \text{if } \text{mod}(\lfloor t \rfloor, 4) = 1; \\ \sum_{\mathbf{x}} V_I(q_{\mathbf{x}+\mathcal{N}}^B, q_{\mathbf{x}}^A) + V_{\text{pin}}(q_{\mathbf{x}}^B) & \text{if } \text{mod}(\lfloor t \rfloor, 4) = 3. \end{cases} \quad (7)$$

Without loss of generality, we set the mass, $m = 1/2$, in the remaining discussions.

IV. DISCRETE TIME-CRYSTAL IN THE π -TOOM MODEL

Within the PCA setting, the π -Toom model (an anti-majority vote in the NEC neighborhood) is a discrete time-crystal, and in the preceding section, we have described a procedure for “simulating” this model using continuous-time Floquet-Langevin dynamics. At zero temperature, $T = 0$, where the dynamics are damped and deterministic, our protocol will faithfully simulate the π -Toom model, as long as the friction coefficient is chosen “correctly” relative to v_I , v_{pin} and the Floquet period. More precisely, one should choose γ to ensure that the oscillators’ relaxation occurs on a time-scale that is short relative to the Floquet period.

The possible flaw at finite temperature is that the errors due to Langevin noise (e.g. thermally activated escape out of the pinning potentials) may not satisfy the requirements of the Gács and Toom error models. Even though Langevin noise is Markovian, the effective error model for our simulated PCA dynamics is not because

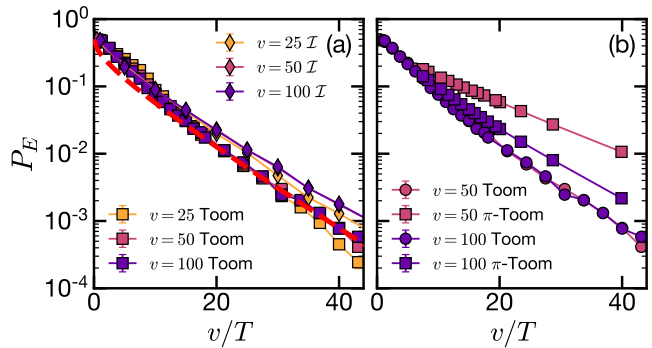


Figure 4. Error probability P_E versus the ratio of the pinning potential to the temperature, v/T , in simulations of (a) the do-nothing (\mathcal{I}) and Toom CAs. The dashed-red line indicates the equilibrium estimate of Eqn. (8). (b) The π -Toom CA. While P_E apparently depends on the simulated CA, as v increases the π -Toom error rate converges toward the Toom error rate. In all cases, we find an exponential decay in the error rate as a function of v/T . Data are obtained from a 32×32 system by averaging over 25 Floquet cycles after an initial evolution of 200 Floquet cycles.

the oscillator-to-CA mapping is many-to-one and thus, the system possesses some extra memory. The worry is that there may then be “avalanches” of errors; for example, if an oscillator makes an error during one step, it *could* be more likely for it to make another error in a subsequent step. Such correlations are harmless so long as they satisfy the bound in Eqn. 2.

We will return to a detailed analysis of error correlations in Sec. V, but let us begin by numerically exploring time crystalline order in a Floquet-Langevin simulation of the π -Toom model.

Consider a binary CA on a two dimensional square lattice, with state-space $\mathcal{S} = \{-1, 1\}$, and a CA-to-oscillator mapping, $Q(s) = s$, as previously discussed. We take the pinning potential to be: $V_{\text{pin}}(q) = v_{\text{pin}}(q-1)^2(q+1)^2 + Fq$, where $F = 10^{-4}$ breaks the accidental Ising symmetry of the π -Toom model. Parameterizing the magnitude of the interaction strength and the pinning potential as $v_{\text{pin}} = 4v_I = v$, we numerically solve the Floquet-Langevin dynamics [Eqn. (3)] via a first-order Euler-stepper. The noise term, $R_i(t)$, is implemented via random momentum kicks with variance $2\eta T dt$, where dt is chosen to ensure that the relative momentum change within each step is small. Finally, γ is chosen such that the dynamics are tuned to critical damping relative to both V_{pin} and V_I .

In order to ensure that a single Floquet period implements only one π -Toom update, we utilize the following interleaving strategy: in step two, we choose $\tilde{\mathcal{T}}$ to be the Toom update rule, while in step four, we choose $\tilde{\mathcal{T}}$ to be the π -Toom update rule. We probe the resulting dynamics by measuring the average “magnetization”, $\langle M_A \rangle \equiv \frac{1}{N} \sum_k \text{sign}(q_k^A)$, where N is the system size. Time crystalline order corresponds to stable period-

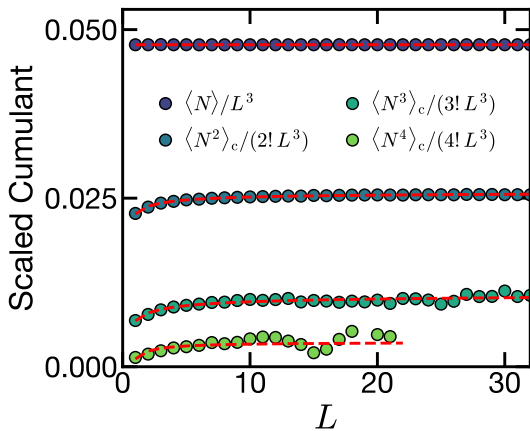


Figure 5. Cumulants, $\langle N^n \rangle_c$, of the error distribution from a Floquet Langevin simulation of the π -Toom model for $L \times L \times L$ space-time volumes. The dashed curves are fits to $\langle N^n \rangle_c / L^3 = c_n - b_n L^{-\eta_n}$. We find $\eta > 0$ (Table I), indicating convergence to a finite c_n . Each data point was estimated from the statistics of 3000 independent Langevin trajectories ($T = 5.17, v = 100$), with 1000 $L \times L \times L$ blocks sampled from each trajectory.

doubling of the magnetization and manifests as a late-time plateau in the order parameter: $(-1)^{\lfloor t/\tau \rfloor} \langle M_A \rangle$.

To investigate the emergence of DTC order, we compute the Floquet-Langevin dynamics starting from three distinct initial states: (i) a uniform input state with all oscillators in $q = +1$ [Fig. 3(a)], (ii) a state which contains an island of $q = -1$ oscillators in the center [Fig. 3(b)], and (iii) a state which consists of diagonal stripes of $q = -1$ oscillators [Fig. 3(c)] [69]. In the language of the π -Toom PCA, for each of these initial states, one can think of the oscillators with $q = -1$ as “errors”, which will either be “corrected” by our Floquet Langevin dynamics (for sufficiently low bath temperatures) or not.

For the uniform initial state [Fig. 3(a)], the DTC order parameter, $(-1)^{\lfloor t/\tau \rfloor} \langle M_A \rangle$, begins at unity for all temperatures. At high temperatures, the order parameter quickly decays to zero, indicating that the Floquet Langevin dynamics drive the system toward the disordered phase. On the other hand, for sufficiently low temperatures, the time crystalline order evolves toward a finite plateau value at late-times, indicative of a DTC. In Fig. 3(b), we show the analogous dynamics starting from an initial state with a central island of errors. For low temperatures, the Floquet Langevin dynamics correct these errors and the DTC order parameter grows, with the system approaching a time crystalline state. Again, above a critical temperature, time crystalline order “melts” and the stroboscopic magnetization decays to zero. Finally, Fig. 3(c) depicts the dynamics starting from a striped error configuration; the qualitative features are identical to Fig. 3(b), although the competition between the DTC phase and the disordered phase is more apparent at intermediate temperatures.

n	c_n	b_n	η_n
1	0.048	0	—
2	0.052	0.007	0.60
3	0.067	0.026	0.46
4	0.088	0.060	0.90

Table I. Fitting parameters for the dashed curves in Fig. 5.

In order to characterize the phase transition between the time crystal and the disordered phase as a function of temperature, we compute the late time Floquet Langevin dynamics up to time-scale, $t \sim 10^4$, starting from a uniform initial state. We define the plateau value of the DTC order parameter as the late-time average of the stroboscopic magnetization, $(-1)^{\lfloor t/\tau \rfloor} \langle M_A \rangle$; in particular, we average $(-1)^{\lfloor t/\tau \rfloor} \langle M_A \rangle$ starting at $t = 3000$ for ~ 500 Floquet cycles and ~ 50 noise realizations.

One can immediately observe the DTC phase transition by plotting the time-crystalline order parameter, $(-1)^{\lfloor t/\tau \rfloor} \langle M_A \rangle$, versus T . However, in order to compare our Floquet Langevin simulation with a direct implementation of the π -Toom PCA, we first translate the temperature, T , to an effective error rate P_E (per space-time cell). To do so, for each temperature, we examine the ensemble of all simulated Langevin trajectories and count the number of errors under the continuous to discrete mapping S ; this allows us to empirically determine the error rate, $P_E(T)$. As shown in Fig. 1(c), the time crystalline order parameter exhibits a sharp phase transition as a function of P_E .

Although there is clearly a phase transition, the question remains: How accurate is the Floquet-Langevin simulation of the π -Toom model? To answer this question, we directly implement the π -Toom PCA, assuming an error rate P_E (associated with the transition for each space-time point) with no correlations in space or time. As depicted in Fig. 1(c), the functional form and location of the DTC phase transition are in excellent agreement between our Floquet Langevin simulation and the π -Toom PCA (with improving agreement for larger pinning potential, v). However, some discrepancy can be seen near the transition, where there is a residual dependence on the pinning potential even as $P_E(T)$ is held fixed. As we will see, this discrepancy arises because the Floquet-Langevin errors are spatio-temporally *correlated*. In order to claim that Toom and Gács’ rigorous PCA results apply to our Floquet Langevin simulation in the thermodynamic limit, a more careful analysis of these error correlations is needed—a task to which we now turn.

V. THE NATURE OF ERRORS IN FLOQUET-LANGEVIN DYNAMICS

Due to the presence of a finite temperature bath, the Floquet-Langevin simulation of the π -Toom model is in-

trinsically noisy. Large thermal fluctuations can lead to an “error” in the subsequent state $\tilde{\eta}(\mathbf{x}, t)$ relative to the noiseless transition $\mathcal{T}(\tilde{\eta}(\mathbf{x} + \mathcal{N}, t - 1))$. Fortunately, our overall goal is to simulate the noisy PCA version of the π -Toom model. However, even then, the distribution of errors arising from the Floquet-Langevin dynamics need not (a priori) be consistent with the error model considered in the context of e.g. Gács’ and Toom’s mathematical results on stability. To this end, we now characterize the nature of errors in our Floquet-Langevin simulation.

Our goal is to obtain numerical evidence that: (1) the errors arising from the Floquet-Langevin dynamics satisfy the condition in Eqn. 2 for some constant $\epsilon(T)$ and (2) the error bound $\epsilon(T)$ can be made arbitrarily small as $T \rightarrow 0$, to ensure the error threshold for Toom or Gács’ results can be obtained.

To begin, we first examine the temperature dependence of the error *rate* per space-time cell $P_E = \langle E_x \rangle$, where $E_x = 0/1$ is the indicator function for an error at x , and show that $P_E(T)$ decays exponentially as $T \rightarrow 0$. Note that due to the spatio-temporal correlation of errors, the error rate is not the same as the error bound, $P_E \neq \epsilon$, but P_E will nevertheless play an important roll in the analysis. In Fig. 4a, we show the empirically measured error rate $P_E(T)$ as a function of v/T for two simulated PCAs which are usually static: the “do-nothing” CA \mathcal{I} and the Toom CA. We find P_E decays exponentially in v/T , suggesting that the errors arise from activated tunneling over the V_{pin}, V_I barriers. For the parameters studied here, we expect the dominant error source arises from the transition between the “Fix A (B) move B (A)” step and the relaxation step enforced by V_I . To predict the rate of such errors, suppose that the interaction potential is driving an oscillator to the state $q = -1$, so that $V_I(q) = \frac{v_I}{2}(q + 1)^2$. When the dynamics switch to the pinning potential $V_{\text{pin}}(q)$, an error will occur if the oscillator has a position $q \in [0, \infty)$. Assuming the system reaches local equilibrium with respect to V_I , the probability of this error can be estimated from the Boltzmann distribution as:

$$P_E\left(\frac{v_I}{T}\right) \equiv \frac{\int_0^\infty e^{-V_I(q)/T} dq}{\int_{-\infty}^\infty e^{-V_I(q)/T} dq} = \frac{1}{2} \text{Erfc}\left(\sqrt{\frac{v_I}{2T}}\right), \quad (8)$$

which asymptotically gives exponential decay $P_E \sim e^{-v_I/2T}$. In Fig. 4a, we show that this prediction (dashed red line) gives good agreement with the observed decay.

In Fig. 4b, we examine $P_E(T)$ for the π -Toom CA, which involves considerable motion during each cycle. For small v_I , the π -Toom CA error rate is higher than the Toom CA, suggesting that non-equilibrium effects beyond the estimate of Eqn. (8) are important. As v increases, the π -Toom error rate approaches that of the static CA. Regardless, in all cases we find that decreasing the temperature leads to an exponential decay in P_E , implying that for strong potentials and low temperatures, arbitrarily small P_E can be obtained.

We now turn to the crucial issue of spatio-temporal correlations. Consider an arbitrary space-time volume V

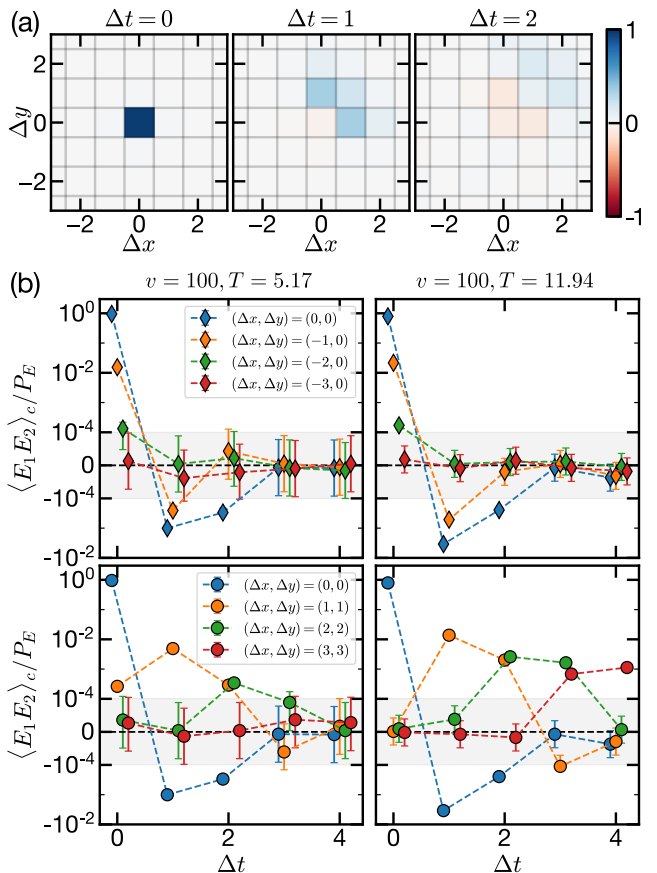


Figure 6. Connected two-point correlations of the errors. (a) Depicts the propagation of errors in real space for $v = 100$ and $T = 5.17$. The connected correlation, $\langle E_1 E_2 \rangle_c / P_E$, for different time separations Δt is shown as a function of the spatial separations. The color map range is rescaled by 1.0, 0.025, 0.004 for the left, middle and right panels respectively. (b) Depicts the connected correlations for different cuts along space (top and bottom) and different temperatures (left and right).

containing $|V|$ points. Letting $P(N_V)$ denotes the probability that N_V errors occur in the volume V , we aim to provide empirical evidence that there is a constant ϵ such that $P(N_V = |V|) \leq \epsilon^{|V|}$ for all V . However, measuring $P(N_V = |V|)$ directly is difficult because for large $|V|$ such “large deviations” [70–73] are too rare to collect statistics. To make progress, we will instead relate $P(N_V = |V|)$ to the connected n -point functions of the errors, which are feasible to estimate for low enough n . Roughly speaking, if the connected n -point functions decay fast enough, the desired bound will be satisfied.

To do so, we consider the scaled cumulant generating function (SCGF) $\lambda_V(k)$ defined by $\langle e^{k N_V} \rangle = e^{|V| \lambda_V(k)}$. The SCGF upper bounds $P(N_V = |V|) \leq e^{-|V|(k - \lambda_V(k))}$ for any choice of $k \geq 0$. The error bound can then be defined by a min-max principle

$$\ln(1/\epsilon) = \min_V \max_{k \geq 0} (k - \lambda_V(k)). \quad (9)$$

The Taylor series of the SCGF gives the n -th cumulants of N_V , $\lambda_V(k) = |V|^{-1} \sum_{n=1}^{\infty} \langle N_V^n \rangle_c \frac{k^n}{n!}$. The cumulants are in turn related to the connected correlations, e.g., $\langle N_V^2 \rangle_c = \sum_{x,y \in V} \langle E_x E_y \rangle_c$. If the correlations decay, we expect the cumulants to scale as $\langle N_V^n \rangle_c = |V| c_n(V)$, where $c_n(V)$ depends on the geometry of V but does not grow with $|V|$ (in particular, $c_1(V) = P_E$). Let us suppose that their growth is upper bounded by a constant $c_n \equiv \max_V c_n(V)$. Furthermore, suppose that the resulting c_n grow slower than $n!$, so that we obtain a bound $\lambda_V(k) \leq \lambda(k) \equiv \sum_{n=1}^{\infty} c_n \frac{k^n}{n!}$ for all $k \geq 0$. It would then follow that $\ln(1/\epsilon) = \max_{k \geq 0} (k - \lambda(k))$. Since $\lambda(0) = 0$ and $\lambda'(k) = P_E < 1$, the maximal value is positive and finite, ensuring Eqn. (2) is satisfied for some $\epsilon < 1$.

Our goal, then, is to provide empirical evidence that $\langle N_V^n \rangle_c$ does not grow faster than $|V|$ or $n!$. Rather than enumerating over all V , we restrict our attention to space-time boxes of dimension $|V| = L \times L \times L$ (note that such compact volumes are the most likely to show violations, as they contain the most correlations). In Fig. 5, we show the estimated cumulants of our Floquet Langevin simulation of the π -Toom model for $L = 2 - 32$. They converge to a finite c_n with a power law correction in $1/L$. While it is difficult to estimate the cumulants beyond $n > 3$, from the available data the $n!$ bound on c_n is safely satisfied.

It is interesting to note that the errors are power-law correlated and non-Gaussian. In Fig. 6, we present data on the two-point correlations $\langle E_{\Delta t, \Delta x, \Delta y} E_{0,0,0} \rangle_c$ of the π -Toom simulation. We see that an initial error causes an increased likelihood for errors at nearby space-time points, with correlations which propagate outward in an anisotropic manner consistent with Toom's NEC-rule. While it is again difficult to obtain estimates for large spatio-temporal separations, if we indulge in fitting three points to a line, the decay is consistent with a power-law, in agreement with the power-law convergence of the cumulants $\langle N^n \rangle_c$.

Finally, we turn to whether the error bound $\epsilon(T) \rightarrow 0$ as $T \rightarrow 0$. One sufficient condition is the existence of a T -independent, continuous, and strictly increasing function $\Lambda(k)$ such that $\lambda(k) \leq P_E(T)\Lambda(k)$ for all $k, T \geq 0$, with $\Lambda(0) = 0$. To see why, note the min-max principle gives

$$\log(1/\epsilon(T)) \geq \max_{k \geq 0} (k - P_E(T)\Lambda(k)). \quad (10)$$

Since Λ is invertible on \mathbb{R}^+ , we may define $k_*(P_E) = \Lambda^{-1}(1/P_E)$. Eqn. (10) then provides the bound $\log(1/\epsilon(T)) \geq k_*(P_E(T)) - 1$. Finally, note $\lim_{P_E \rightarrow 0} k_*(P_E) = \infty$, because the inverse of a strictly increasing function is itself strictly increasing. Thus, the existence of such a $\Lambda(k)$, combined with our earlier evidence that $\lim_{T \rightarrow 0} P_E(T) = 0$, would imply $\lim_{T \rightarrow 0} \epsilon(T) = 0$.

To verify the existence of such a $\Lambda(k)$, it would be sufficient to show that the scaled cumulants are bounded as $c_n(T) \leq P_E(T)C_n$, with C_n growing slower than $n!$, so that $\Lambda(k)$ has an infinite radius of convergence (Poisson

statistics corresponds to $C_n = 1$, $\Lambda(k) = e^k$). However, due to the small statistics, numerically estimating c_n at low temperatures is extremely demanding. A preliminary comparison of $T = 5.17, 11.94$ (see appendix A) finds $c_2(T)/P_E(T) = 1.24$ at $T = 11.94$, while $c_2(T)/P_E(T) = 1.08$ at $T = 5.17$, consistent with an approach to $C_2 \sim 1$, but a comprehensive investigation remains a work in progress.

In summary, despite errors which are power-law correlated and non-Gaussian, we find compelling evidence that Langevin-Floquet dynamics can simulate a PCA with an error bound $\epsilon(T)$ that satisfies Eq. (2), so that Toom and Gács' results may be applied to this setting. Of course we cannot rule out that for some anomalously large volume $|V|$, cumulant order n , or inverse temperature $1/T$, the observed behavior will change course and violate the bound—a caveat common to any numerical finite-scaling approach. Obtaining a rigorous proof of this bound thus remains an interesting future direction.

VI. DISCUSSION AND OUTLOOK

There is a long history of understanding computation as a fundamentally physical process, and the subsequent constraints which arise from thermodynamics: “Computers may be thought of as engines for transforming free energy into waste heat and mathematical work” [67, 74, 75]. In this point of view, a time-crystal can be understood as a physical realization of the second-simplest possible computer program: a global NOT-gate. By demanding that the program execute perfectly despite faulty (noisy) gates, and when restricting to physical implementations that rely only on local interactions, the execution of such a program can be understood as a non-equilibrium “phase of matter,” and the error threshold as a non-equilibrium phase transition into a time-crystalline phase.

It is interesting to speculate about extensions of this approach to the quantum setting, where a discrete-time Markov process is promoted to a quantum channel, and the Langevin bath to a Lindbladian. On the one hand, any classical Markov process, such as the Toom or Gács PCA, can be realized as a quantum channel which dephases and acts diagonally on populations. When assessing stability in the quantum setting, however, it remains to be shown that the ergodicity breaking is robust to imperfect dephasing. On the other hand, error-corrected quantum computing can be realized as a purely local autonomous process in the thermodynamic limit [76, 77] and by analogy to the discussion above, one may realize a time-crystal by running the program “NOT” on an error-corrected quantum computer. In this sense, the existence of time-crystals in open systems is an elementary application of deeper results regarding the physical possibility of error-correction in autonomous, locally interacting systems.

Acknowledgements—We are greatly indebted to conversations with P. Gács for generously explaining various

details of his work, C. Maes for pointing us to the literature on coupled map lattices, and C. Nayak and L. Balents for collaborations on related work. MPZ is indebted to conversations with D. Huse during the initiation of this work. This work is supported in part by the Army Re-

search Office (Grant No. W911NF2110262), the DARPA DRINQS program (Grant No. D18AC00033), the A. P. Sloan foundation, the David and Lucile Packard foundation, and the W. M. Keck Foundation.

-
- [1] A. C. Potter, T. Morimoto, and A. Vishwanath, *Phys. Rev. X* **6**, 041001 (2016).
- [2] V. Khemani, A. Lazarides, R. Moessner, and S. L. Sondhi, *Phys. Rev. Lett.* **116**, 250401 (2016).
- [3] D. V. Else, B. Bauer, and C. Nayak, *Phys. Rev. Lett.* **117**, 090402 (2016).
- [4] N. Y. Yao, A. C. Potter, I.-D. Potirniche, and A. Vishwanath, *Phys. Rev. Lett.* **118**, 030401 (2017).
- [5] J. Zhang, P. Hess, A. Kyprianidis, P. Becker, A. Lee, J. Smith, G. Pagano, I.-D. Potirniche, A. C. Potter, A. Vishwanath, *et al.*, *Nature* **543**, 217 (2017).
- [6] S. Choi, J. Choi, R. Landig, G. Kucsko, H. Zhou, J. Isoya, F. Jelezko, S. Onoda, H. Sumiya, V. Khemani, *et al.*, *Nature* **543**, 221 (2017).
- [7] D. V. Else, C. Monroe, C. Nayak, and N. Y. Yao, *Annual Review of Condens. Matter Phys.* **11**, 467 (2020).
- [8] R. Nandkishore and D. A. Huse, *Annu. Rev. Condens. Matter Phys.* **6**, 15 (2015).
- [9] P. Ponte, Z. Papić, F. Huveneers, and D. A. Abanin, *Phys. Rev. Lett.* **114**, 140401 (2015).
- [10] D. A. Abanin, E. Altman, I. Bloch, and M. Serbyn, *Rev. Mod. Phys.* **91**, 021001 (2019).
- [11] J. A. Kjäll, J. H. Bardarson, and F. Pollmann, *Phys. Rev. Lett.* **113**, 107204 (2014).
- [12] M. Bukov, L. D'Alessio, and A. Polkovnikov, *Adv. Phys.* **64**, 139 (2015).
- [13] D. A. Abanin, W. De Roeck, and F. Huveneers, *Ann. Phys.* **372**, 1 (2016).
- [14] S. A. Weidinger and M. Knap, *Sci. Rep.* **7**, 1 (2017).
- [15] D. A. Huse, R. Nandkishore, V. Oganesyan, A. Pal, and S. L. Sondhi, *Phys. Rev. B* **88**, 014206 (2013).
- [16] A. Chandran, V. Khemani, C. Laumann, and S. L. Sondhi, *Phys. Rev. B* **89**, 144201 (2014).
- [17] Y. Bahri, R. Vosk, E. Altman, and A. Vishwanath, *Nat. Commun.* **6**, 7341 (2015).
- [18] I.-D. Potirniche, A. C. Potter, M. Schleier-Smith, A. Vishwanath, and N. Y. Yao, *Phys. Rev. Lett.* **119**, 123601 (2017).
- [19] D. A. Abanin, W. De Roeck, and F. Huveneers, *Phys. Rev. Lett.* **115**, 256803 (2015).
- [20] D. V. Else, B. Bauer, and C. Nayak, *Phys. Rev. X* **7**, 011026 (2017).
- [21] T.-S. Zeng and D. Sheng, *Phys. Rev. B* **96**, 094202 (2017).
- [22] T. Mori, *Phys. Rev. B* **98**, 104303 (2018).
- [23] F. Machado, G. D. Kahanamoku-Meyer, D. V. Else, C. Nayak, and N. Y. Yao, *Phys. Rev. Research* **1**, 033202 (2019).
- [24] F. Machado, D. V. Else, G. D. Kahanamoku-Meyer, C. Nayak, and N. Y. Yao, *Phys. Rev. X* **10**, 011043 (2020).
- [25] A. Kyprianidis, F. Machado, W. Morong, P. Becker, K. S. Collins, D. V. Else, L. Feng, P. W. Hess, C. Nayak, G. Pagano, *et al.*, *Science* **372**, 1192 (2021).
- [26] B. Ye, F. Machado, and N. Y. Yao, *Phys. Rev. Lett.* **127**, 140603 (2021).
- [27] A. Pizzi, A. Nunnenkamp, and J. Knolle, *Phys. Rev. Lett.* **127**, 140602 (2021).
- [28] D. V. Else, W. W. Ho, and P. T. Dumitrescu, *Phys. Rev. X* **10**, 021032 (2020).
- [29] A. Lasota, T.-Y. Li, and J. Yorke, *Transactions of the American Mathematical Society* **286**, 751 (1984).
- [30] J. Losson, J. Milton, and M. C. Mackey, *Physica D* **81**, 177 (1995).
- [31] J. Losson and M. C. Mackey, *Stochastic and spatial structures of dynamical systems*, 41 (1996).
- [32] G. Gielis and R. MacKay, *Nonlinearity* **13**, 867 (2000).
- [33] U. Parlitz, L. Junge, and L. Kocarev, *Phys. Rev. Lett.* **79**, 3158 (1997).
- [34] N. Y. Yao, C. Nayak, L. Balents, and M. P. Zaletel, *Nat. Phys.* **16**, 438 (2020).
- [35] V. Khemani, R. Moessner, and S. Sondhi, arXiv preprint arXiv:1910.10745 (2019).
- [36] K. Kaneko, *Progress of Theoretical Physics* **72**, 480 (1984).
- [37] R. Kapral, *Phys. Rev. A* **31**, 3868 (1985).
- [38] L. A. Bunimovich and Y. G. Sinai, *Nonlinearity* **1**, 491 (1988).
- [39] K. Kaneko, *Chaos: An Interdisciplinary Journal of Non-linear Science* **2**, 279 (1992).
- [40] K. Kaneko and T. Konishi, *J. Phys. Soc. Jpn.* **56**, 2993 (1987).
- [41] J. Von Neumann, in *Systems Research for Behav. Sci.s* (Routledge, 1968) pp. 97–107.
- [42] S. Wolfram, *Rev. Mod. Phys.* **55**, 601 (1983).
- [43] P. Gács, *J. Stat. Phys.* **103**, 45 (2001).
- [44] L. F. Gray, *J. Stat. Phys.* **103**, 1 (2001).
- [45] A. L. Toom, *Advances in Probability* **6**, 549 (1980).
- [46] C. H. Bennett and G. Grinstein, *Phys. Rev. Lett.* **55**, 657 (1985).
- [47] D. Makowiec, *Phys. Rev. E* **60**, 3787 (1999).
- [48] G. Grinstein, *IBM Journal of Research and Development* **48**, 5 (2004).
- [49] S. Ulam *et al.*, in *Proceedings of the International Congress on Mathematics*, Vol. 2 (Citeseer, 1952) pp. 264–275.
- [50] J. Neumann, A. W. Burks, *et al.*, *Theory of self-reproducing automata*, Vol. 1102024 (University of Illinois press Urbana, 1966).
- [51] A. L. Toom, *Problemy Peredachi Informatsii* **10**, 70 (1974).
- [52] D. Dawson, *Information and Control* **34**, 93 (1977).
- [53] P. Gács, *Journal of Computer and System Sciences* **32**, 15 (1986).
- [54] P. Gacs, arXiv preprint arXiv:2105.05968 (2021).
- [55] E. F. Codd, *Cellular automata* (Academic press, 2014).
- [56] C. H. Bennett, G. Grinstein, Y. He, C. Jayaprakash, and D. Mukamel, *Phys. Rev. A* **41**, 1932 (1990).

- [57] O. Perron, *Mathematische Annalen* **64**, 248 (1907).
- [58] G. Frobenius, F. G. Frobenius, F. G. Frobenius, F. G. Frobenius, and G. Mathematician, (1912).
- [59] J. Randall, C. Bradley, F. van der Gronden, A. Galicia, M. Abobeih, M. Markham, D. Twitchen, F. Machado, N. Yao, and T. Taminiau, arXiv preprint arXiv:2107.00736 (2021).
- [60] X. Mi, M. Ippoliti, C. Quintana, A. Greene, Z. Chen, J. Gross, F. Arute, K. Arya, J. Atalaya, R. Babbush, *et al.*, arXiv preprint arXiv:2107.13571 (2021).
- [61] W. De Roeck and F. Huveneers, *Phys. Rev. B* **95**, 155129 (2017).
- [62] P. J. Crowley and A. Chandran, *Phys. Rev. Research* **2**, 033262 (2020).
- [63] I. Enting, *J. Phys. C: Solid State Phys.* **10**, 1379 (1977).
- [64] E. Domany and W. Kinzel, *Phys. Rev. Lett.* **53**, 311 (1984).
- [65] N. Privault, *Examples and Applications*, Publisher Springer-Verlag Singapore **357**, 358 (2013).
- [66] P. Lencastre, F. Raischel, T. Rogers, and P. G. Lind, *Phys. Rev. E* **93**, 032135 (2016).
- [67] D. H. Wolpert, *J. Phys. A: Math. Theor.* **52**, 193001 (2019).
- [68] Naively, one could set $\tilde{\mathcal{T}}(\{q_{\mathbf{x}+\mathcal{N}}^A\}) = Q(\mathcal{T}(S(q_{\mathbf{x}+\mathcal{N}}^A)))$. However, the discontinuities in $S(q)$, and hence V_I , lead to isolated points with infinite force, which makes any analysis or numerical simulation significantly more troublesome. To remedy this, we smooth the interaction using an interpolation as detailed in Appendix A.
- [69] Note that for perfect stripes, even the deterministic Toom model cannot not correct it. However, there are a measure zero set of such fine-tuned initial conditions.
- [70] J.-D. Deuschel and D. W. Stroock, *Large deviations*, Vol. 342 (American Mathematical Soc., 2001).
- [71] S. S. Varadhan, *Large deviations and applications* (SIAM, 1984).
- [72] F. Den Hollander, *Large deviations*, Vol. 14 (American Mathematical Soc., 2008).
- [73] H. Touchette, arXiv preprint arXiv:1106.4146 (2011).
- [74] R. Landauer, *IBM J. Res. Dev.* **5**, 183 (1961).
- [75] C. H. Bennett, *InterNatl. J. (Wash.) of Theoretical Physics* **21**, 905 (1982).
- [76] J. W. Harrington, *Analysis of quantum error-correcting codes: symplectic lattice codes and toric codes* (California Institute of Technology, 2004).
- [77] G. Dauphinais and D. Poulin, *Commun. Math. Phys.* **355**, 519 (2017).

Appendix A: Details of the Floquet Langevin Evolution and Numerical Simulation

In the “fix A , move B ” step, if we fix the A oscillators, then the B oscillators are critically damped harmonic oscillators with additional noise. If there is no noise, then replacing $q_k^B = \exp(\lambda t)$ gives two eigenvalues $\lambda = -(1/2) \left(\gamma \pm \sqrt{\gamma^2 - 4v_I} \right)$. Thus, the decay of oscillation amplitude is fastest when the damping has the critical value $\gamma^* = 2\sqrt{v_I}$. When $\gamma > \gamma^*$, it is over-damped, and the relaxation is slow because the velocity is low. When $\gamma < \gamma^*$, oscillation remain and the damping is slow due

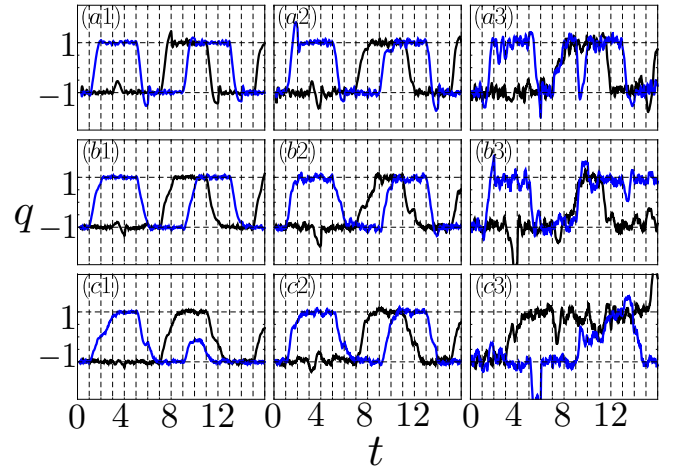


Figure 7. Error correction process in Floquet Langevin simulation of the π -Toom model. Dynamics are shown for a 32×32 lattice with a pinning potential $v = 50$. The blue lines represent the A oscillator and the black lines represent the B oscillator. From left to right, the temperature is varied such that $T = 0.5, 2, 10$. From top to bottom, we change the damping ratio, $\kappa_f = 0.5, 1, 1.5$

to small friction coefficient. Similarly, in the “relaxation” steps, both oscillators correspond to damped harmonic oscillators for the potential $V_{\text{pin}}(q) = v_{\text{pin}}(q^2 - 1)^2 \simeq 4v_{\text{pin}}(q - 1)^2$ near $q = +1$. The critical damping during the relaxation step is then given by $\gamma_r^* = 4\sqrt{2v_{\text{pin}}}$. We tune the damping ratio $\kappa_f = \gamma/\gamma^* = \gamma_r/\gamma_r^*$ such all steps within the Floquet evolution are tuned to critical damping. For simplicity, we let $v_{\text{pin}} = 4v_I = v$, and then the critical relaxation time when $\kappa_f = 1$ is $t_r^* \sim 1/\sqrt{v}$. The critical damped solution when the initial oscillator position is q_0 at rest is given by $q(t) = q_0 e^{-\sqrt{v}t} (\sqrt{v}t + 1)$.

First, we verify the correction of a single error under π -Toom dynamics. To do so, we set the initial position of the A , B oscillators to be uniformly $q = +1$ in all cells, except at cell $(1, 1)$, where we choose $q = -1$ to create an error. All initial momenta are zero. In Fig. 8, we monitor the position of the A and B oscillator at cell $(1, 1)$. In this plot, between $[0, 1]$, $[2, 3]$, $[4, 5]$, \dots we have the relaxation steps; between $[1, 2]$, $[5, 6]$, $[9, 10]$, \dots , we have Toom steps; while between $[3, 4]$, $[7, 8]$, $[11, 12]$, \dots we have π -Toom steps. We see that in all cases the error gets corrected within a duration of $t = 4$, after which the black and blue curves have similar shapes at low temperature; however, the critical damping case [Fig. 8(b1-b3)] relaxes the fastest and exhibits the smallest fluctuations, compared with the under-damped [Fig. 8(a1-a3)] and over-damped [Fig. 8(c1-c3)] cases. We have verified that the same behavior holds for various pinning potentials v and temperatures T .

Smoothing discontinuities—The interaction V_I in Eqn. (5) involves two set of coordinates: $q_{\mathbf{x}}^B$ and $\{q_{\mathbf{x}+\mathcal{N}}^A\}$. In the numerical simulation, one needs to implement the motion by applying a force on the A oscillators and B

oscillators. Naively, the \tilde{T} of Eqn. (5) would be taken as $Q(\mathcal{T}(S(q)))$. However, due to the discontinuities in S , this choice would cause V_I to depend discontinuously on $\{q_{\mathbf{x}+\mathcal{N}}^A\}$, leading to δ -function forces. This would make the numerical simulation of Hamilton's equations challenging. To avoid this, we first evaluate the values of V_I at a discrete set of points of $q_{\mathbf{x}+\mathcal{N}}^A = \pm 1$, while keeping $q_{\mathbf{x}}^B$ arbitrary. We then create a linear interpolation between these discrete points to create a smoothed version of V_I for oscillators A , which allows the evaluation of the force in the numerical simulation.

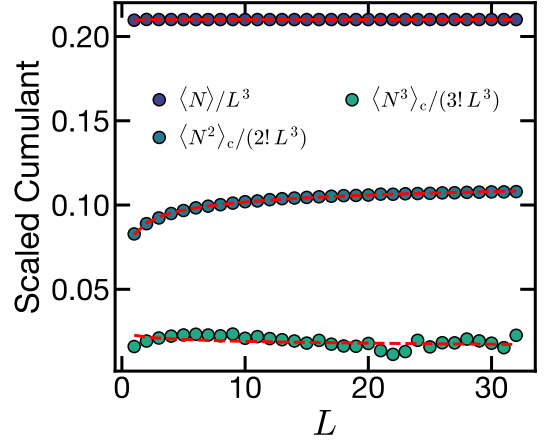


Figure 8. Cumulants, $\langle N_V^n \rangle_c$, of the error distribution from a Floquet Langevin simulation of the π -Toom model for $T = 11.94, v = 100$. Using the same fitting functional form as in Figure 5, we find $c_1 = 0.21$ and $c_2 = 0.26$. We find that accurately estimating higher cumulants, e.g. c_3 and c_4 , is more challenging at temperatures above the critical temperature, $T_c = 9.6$.